Gadolinium Retention in the Dentate Nucleus and Globus Pallidus Is Dependent on the Class of Contrast Agent[1]

Alexander Radbruch, MD, JD
Lukas D. Weberling
Pascal J. Kieslich, MSc
Oliver Eidel
Sina Burth
Philipp Kickingereder, MD
Sabine Heiland, PhD
Wolfgang Wick, MD
Heinz-Peter Schlemmer, MD, PhD
Martin Bendszus, MD

Purpose: To compare changes in signal intensity (SI) ratios of the dentate nucleus (DN) and the globus pallidus (GP) to those of other structures on unenhanced T1-weighted magnetic resonance (MR) images between linear and macrocyclic gadolinium-based contrast agents (GBCAs).

Materials and Methods: The study was approved by the ethical committee of the University of Heidelberg (reference no. S-324/2014). Owing to the retrospective character of the study, the ethical committee did not require any written informed consent. Two groups of 50 patients who underwent at least six consecutive MR imaging examinations with the exclusive use of either a linear GBCA (gadopentetate dimeglumine) or a macrocyclic GBCA (gadoterate meglumine) were analyzed retrospectively. The difference in mean SI ratios of DN to pons and GP to thalamus on unenhanced T1-weighted images from the last and first examinations was calculated. One-sample and independent-sample *t* tests were used to assess the difference in SI ratios for both groups, and regression analysis was performed to account for potential confounders.

Results: The SI ratio difference in the linear group was greater than 0 (mean DN difference ± standard deviation, 0.0407 ± 0.0398 [$P < .001$]; GP, 0.0287 ± 0.0275 [$P < .001$]) and significantly larger (DN, $P < .001$ and standardized difference of 1.16; GP, $P < .001$ and standardized difference of 0.81) than that in the macrocyclic group, which did not differ from 0 (DN, 0.0016 ± 0.0266 [$P = .680$]; GP, 0.0031 ± 0.0354 [$P = .538$]). The SI ratio difference between the last and first examinations for the DN remained significantly different between the two groups in the regression analysis ($P < .001$).

Conclusion: This study indicates that an SI increase in the DN and GP on T1-weighted images is caused by serial application of the linear GBCA gadopentetate dimeglumine but not by the macrocyclic GBCA gadoterate meglumine. Clinical implications of this observation remain unclear.

[1] From the Department of Neuroradiology, University of Heidelberg Medical Center, Im Neuenheimer Feld 400, 69120 Heidelberg, Germany (A.R., L.D.W., O.E., S.B., P.K., S.H., M.B.); Department of Radiology, German Cancer Research Center (DKFZ), Heidelberg, Germany (A.R., H.P.S.); Department of Psychology, University of Mannheim, Mannheim, Germany (P.J.K.); and Neurology Clinic, University of Heidelberg, Heidelberg, Germany (W.W.). Received February 10, 2015; revision requested February 23; revision received March 9; accepted March 15; final version accepted March 17. Supported by Guerbet. **Address correspondence to** A.R. (e-mail: *Alexander.Radbruch@med.uni-heidelberg.de*).

Investigators in three recently published studies (Kanda et al [1] [2014], Errante et al [2], and Kanda et al [3] [2015]) reported increased signal intensities (SIs) in the dentate nucleus (DN) on unenhanced T1-weighted magnetic resonance (MR) images after serial application of gadolinium-based contrast agent (GBCA) for contrast material–enhanced MR imaging. The authors of these studies suggested a deposition of gadolinium in the DN as a possible cause of the increased SI on unenhanced T1-weighted images.

Free gadolinium is highly toxic, which is why it needs to be bound to a ligand for its use as a contrast agent (4). Hence, one mechanism underlying the potential toxic effects of GBCAs is the release of gadolinium ions (Gd^{3+}) from the complex and its deposition in tissues. This potential release of Gd^{3+} ions depends on the stability of the GBCA in a biologic environment, the physicochemical properties, and the chemical structure of the gadolinium complex. In this respect, commercially available gadolinium complexes can be divided into two major classes: linear and macrocyclic complexes (Fig 1) (5,6). Several investigators have found an increased release of Gd^{3+} ion in vitro from linear GBCAs compared with macrocyclic GBCAs, as well as a higher deposition rate in some tissues in vivo (6,7). These findings suggest that the occurrence of increased SI in the DN after serial application of contrast agents may result from a local Gd^{3+} ion deposition and depend on the class of GBCA used.

In Kanda et al (3), the authors provide evidence that SI increase in the DN on unenhanced T1-weighted MR images is associated with the previous administration of the linear GBCA gadopentetate dimeglumine (Magnevist; Bayer), but not with the macrocyclic GBCA gadoteridol (ProHance; Bracco Spa, Milano, Italy). However, the statistical power of this study was limited because of the low number of included patients with proven hyperintensity on unenhanced T1-weighted images in the DN (nine patients) and the absence of a longitudinal comparison of SIs in patients who received high numbers of previous GBCA administrations.

In the current study, we investigated two large patient cohorts who underwent at least six serial MR imaging examinations to compare changes in SI ratios of the DN and the globus pallidus (GP) to those of other structures on unenhanced T1-weighted MR images between linear and macrocyclic GBCAs.

Advances in Knowledge

- Increased signal intensities (SIs) in the dentate nucleus (DN) and globus pallidus (GP) on unenhanced T1-weighted images are related to the serial application of the linear gadolinium-based contrast agent (GBCA) gadopentetate dimeglumine ($P < .001$ for both DN and GP).
- No significant SI increase could be demonstrated after serial applications of the macrocyclic GBCA gadoterate meglumine ($P = .680$ for DN, $P = .538$ for GP).
- The SI increase of the DN depends on the accumulated dose of the applied GBCA in the gadopentetate dimeglumine group ($P = .001$).

Materials and Methods

This retrospective study was financially supported by Guerbet. The authors of this study had full control of the data and the information submitted for publication.

Patients

The study was approved by the ethical committee of the University of Heidelberg (reference no. S-324/2014). Because of the retrospective character of the study, the ethical committee did not require any written informed consent. All patients had given consent to the use of their image data at the time of the examination.

Our in-house radiologic information system was screened for consecutive patients until two groups of 50 consecutive patients were identified who underwent at least six consecutive MR imaging examinations by using exclusively linear GBCAs (gadopentetate dimeglumine, Magnevist; Bayer) or macrocyclic GBCAs (gadoterate meglumine, Dotarem; Guerbet) and who fulfilled inclusion criteria and did not fulfill the exclusion criteria.

Inclusion criteria were the following: *(a)* at least six consecutive gadolinium-enhanced MR imaging examinations were performed with exclusively linear GBCAs or exclusively macrocyclic GBCAs as the contrast agent and *(b)* all of those consecutive MR imaging examinations were performed exclusively in our department. Included MR imaging examinations did not have to be the first examinations in which GBCAs were used, and prior gadolinium-enhanced examinations might have been performed at

Implication for Patient Care

- Even though no clinical implications can be drawn from the reported hyperintensities in the DN and the GP, the findings are worrisome and should be taken into account when deciding whether to use gadopentetate dimeglumine.

Published online before print
10.1148/radiol.2015150337 **Content codes:** MR NR

Radiology 2015; 275:783–791

Abbreviations:
CI = confidence interval
CSF = cerebrospinal fluid
DN = dentate nucleus
eGFR = estimated glomerular filtration rate
GBCA = gadolinium-based contrast agent
GP = globus pallidus
SI = signal intensity

Author contributions:
Guarantors of integrity of entire study, A.R., H.P.S.; study concepts/study design or data acquisition or data analysis/interpretation, all authors; manuscript drafting or manuscript revision for important intellectual content, all authors; approval of final version of submitted manuscript, all authors; agrees to ensure any questions related to the work are appropriately resolved, all authors; literature research, A.R., L.D.W., S.H., H.P.S., M.B.; clinical studies, A.R., L.D.W., P.K., S.H.; experimental studies, A.R., L.D.W.; statistical analysis, A.R., L.D.W., P.J.K., P.K., M.B.; and manuscript editing, all authors

Conflicts of interest are listed at the end of this article.

See also the article by McDonald et al and the editorial by Kanal and Tweedle in this issue.

Figure 1

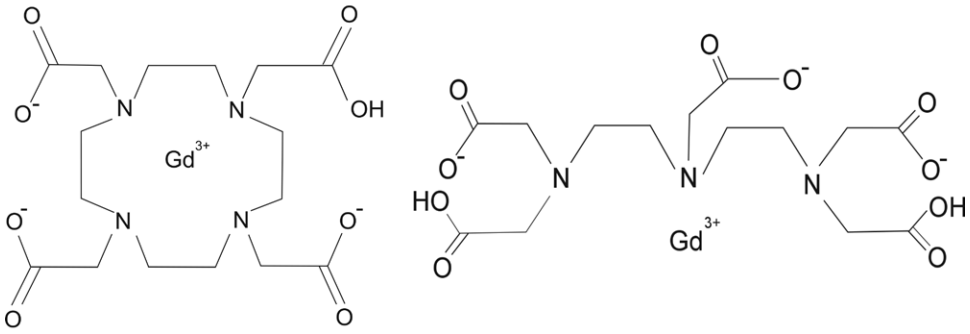

Figure 1: Diagrams of **(a)** the chemical structure of the macrocyclic GBCA gadoterate meglumine (Dotarem; Guerbet, Paris, France) and **(b)** the linear GBCA gadopentetate dimeglumine (Magnevist; Bayer, Leverkusen, Germany). Generally, macrocyclic ligands form a rigid cage with a preorganized cavity to fit the coordination sphere of the Gd^{3+} ion, while linear ligands wrap around the Gd^{3+} ions, forming a more flexible chelate, since the cages are not fully closed.

our institution that were not included owing to the presence of exclusion criteria. Exclusion criteria were *(a)* an estimated glomerular filtration rate (eGFR) lower than 60 mL/min per 1.73 m^2 in a blood sample recent to the date of the last MR imaging examination; *(b)* a history of brain hemorrhage, stroke, or brain ischemia; *(c)* edema, tumor, or other lesions located in the cerebellum or pons; *(d)* history of intracranial infection, such as meningitis or encephalitis; *(e)* missing or unsatisfactory unenhanced T1-weighted MR images (eg, largely varying MR parameters) from the first or last MR imaging examination performed with linear GBCAs or macrocyclic GBCAs; and *(f)* missing documentation of the contrast agent applied. Table 1 lists the number of patients excluded owing to each of the exclusion criteria.

Table 1

Exclusion Criteria

Parameter	Macrocyclic GBCA Group	Linear GBCA Group
Initially selected	64	81
Excluded because of renal dysfunction (eGFR < 60 mL/min per square meter)	2	3
Excluded because of history of brain hemorrhage, stroke, or brain ischemia	4	3
Excluded because of lesions in the pons or cerebellum	2	2
Excluded because of a history of intracranial infections	1	3
Excluded because of missing or unsatisfactory unenhanced T1-weighted images	1	10
Excluded because of missing documentation of the contrast agent	4	0
Excluded because of different sequences used to obtain T1-weighted images	0	10
Final no. of patients	50	50

Note.—Data are numbers of patients.

Data Analysis

Eighty-one consecutively examined patients who underwent at least six consecutive MR imaging examinations with linear GBCAs and 64 patients who underwent at least six examinations with macrocyclic GBCAs were assessed to identify 50 patients in each group who fulfilled the inclusion and exclusion criteria (Table 1). All patients in the linear GBCA group underwent their last MR imaging examination in the time period from 6 AM on December 8, 2008, to 6 PM on January 31, 2009, and all patients in the macrocyclic GBCA group underwent their last MR imaging examination in the time interval from 10 AM on August 25, 2014, to 11 PM on September 30, 2014. The different time periods in which the data of the different groups were collected are explained by the fact that both GBCAs were preponderantly used at different time periods in our clinic.

For all included patients, age, sex, diagnosis, liver function, and eGFR were evaluated by means of chart review (Table 2). Diagnosis was further specified as *(a)* glioblastoma World Health Organization, or WHO, grade IV, *(b)* glioma WHO grade I–III, *(c)* brain tumor other than glioma WHO grade I–IV, such as cerebral lymphoma, and *(d)* no tumor. For all included patients, it was further assessed whether molecularly targeted therapy (eg, bevacizumab) or alkylating antineoplastic chemotherapy were applied. Furthermore, it was assessed whether patients were treated with whole-brain or tumor-selective brain radiation. Renal function was evaluated by calculating

Table 2

Patient Characteristics of Macrocyclic and Linear GBCA Groups

Parameter	Macrocyclic GBCA Group	Linear GBCA Group
Total no. of patients	50	50
Age (y)*	49.98 ± 14.09	46.78 ± 15.18
Mean interval between GBCA administrations (wk)*	11.28 ± 2.47	14.00 ± 6.19
Patient sex		
No. of men	27	30
No. of women	23	20
No. of contrast-enhanced MR imaging examinations*	7.06 ± 1.20	7.32 ± 1.83
Accumulated dose*	162.41 ± 45.20	124.22 ± 39.31
History of surgery	37	37
History of chemotherapy	46	41
Molecularly targeted therapy	12	12
Alkylating antineoplastic agent	46	37
Other therapy	16	20
Underwent radiation therapy	44	32
Whole brain	2	2
Tumor selective	42	31
Diagnosis		
Glioblastoma	16	13
Glioma World Health Organization grade I–III	31	27
Tumor other than glioma	2	8
No tumor	1	2
eGFR		
60–90 mL/min per 1.73 m^2	12	9
>90 mL/min per 1.73 m^2	38	41
Abnormal liver function	12	15

Note.—Data are numbers of patients, unless indicated otherwise.

* Data are means ± standard deviations.

the eGFR from a recent blood sample, on the basis of the Chronic Kidney Disease Epidemiology Collaboration formula. All patients with an eGFR less than 60 mL/min per 1.73 m^2 were excluded. For the included patients, it was assessed whether the eGFR was *(a)* less than 90 mL/min per 1.73 m^2 or *(b)* more than 90 mL/min per 1.73 m^2. Abnormal liver function was defined by abnormal serum concentrations of alanine aminotransferase, γ-glutamyl transpeptidase, or aspartate aminotransferase. Since the applied linear GBCA and macrocyclic GBCA are both eliminated exclusively by the kidneys, patients with abnormal liver function were not excluded from our study. Finally, the mean interval between GBCA administrations was calculated by dividing the time (in weeks) between the first and last MR imaging examinations by the total number of MR imaging examinations minus 1.

MR Imaging Protocol

MR imaging was performed with a 3-T imaging unit (Trio and/or Verio; Siemens, Erlangen, Germany) or a 1.5-T imaging unit (Symphony; Siemens). The standard MR imaging protocol included an axial T1-weighted spin-echo sequence (repetition time msec/echo time msec, 500/14; section thickness, 6 mm) or a T1-weighted three-dimensional magnetization-prepared rapid gradient-echo sequence (1740/3.45; section thickness, 1.0 mm; field of view, 250 mm) before and after GBCA injection, T2-weighted imaging (4890/85; section thickness, 5 mm; field of view, 230 mm), and a fluid-attenuated inversion-recovery sequence (8500/85; inversion time, 2400 msec; section thickness, 5 mm; and field of view, 230 mm).

Because of the introduction of perfusion-weighted MR imaging in the tumor protocol with a prebolus design (8) after 2010, the applied dose of GBCA differed between groups. There was an exclusive application of a standardized single dose of 15–20 mL in the linear GBCA group and a double injection of GBCA in most of the patients with tumors in the macrocyclic GBCA group. The injected dose of macrocyclic GBCA was adapted to 0.1 mmol per kilogram of the patient's body weight. These different application schemes resulted in a substantially larger dose of the macrocyclic GBCA per MR imaging session (mean dose ± standard deviation, 27.07 mL ± 6.86 per MR imaging examination) compared with the linear GBCA (19.62 mL ± 1.74 per MR imaging examination).

Image Analysis

Image analysis was conducted as described previously by Kanda et al (1,3), but we added the cerebrospinal fluid (CSF) as an additional validator. Thus, the DN SI was compared with that of three structures: the pons, CSF, and cerebellum. All images were reviewed on our picture archiving and communication system. A region of interest was drawn on the unenhanced T1-weighted images on the central pons, the CSF of the fourth ventricle, the cerebellum next to the DNs, and the right and left DNs. To assess the GP, regions of interest were drawn on the GP, as well as on the thalamus. To guarantee a correct placement of the region of interest, T2-weighted images were additionally used for the identification of the DN. The image analysis was performed by a radiologist (A.R.) with 6 years of experience, who was blinded to the clinical data. In contrast to Kanda et al (1,3), who assessed only one DN, GP, and thalamus, we calculated the mean of the left and the right GP, cerebellum, and DN to improve accuracy.

Statistical Analysis

Analyses were conducted by using the R language and environment for statistical computing (version 3.1.0, R Foundation for Statistical Computing,

Vienna, Austria), and the a priori significance level was set to P less than .05. One-sample t tests were used to examine whether the mean SI ratio differences between the last and first examination in each patient group were different from 0, and Jeffreys-Zellner-Siow Bayes factors were computed to quantify the strength of evidence in favor of the null hypothesis (no difference from 0) or the alternative hypothesis (difference from 0) (9). An independent-sample t test was used to test whether the differences between the two patient groups were statistically significant. These analyses were conducted for the DN-to-pons ratio, the DN-to-CSF ratio, the DN-to-cerebellum ratio, and the GP-to-thalamus ratio. For the DN-to-pons ratio, which has mostly been used in previous studies (1,2), additional analyses were conducted: Regression analyses were used to examine whether the differences between groups remained significant after accounting for potential confounding variables. Correlation analyses were used to test whether the number of contrast-enhanced MR imaging examinations, the mean interval between GBCA administrations, and the accumulated dose of GBCA had a different influence in each patient group, supplementing the analysis with Jeffreys-Zellner-Siow Bayes factors to quantify the strength of evidence (10).

Since the sequences used for T1-weighted MR imaging examinations differed in the linear GBCA group (31 magnetization-prepared rapid gradient-echo sequences and 19 spin-echo sequences), a subgroup analysis with an independent sample t test was performed to examine whether the sequences had an influence on the SI ratio difference.

Results

The characteristics of each group are described in Table 2, and the distribution of SI ratio differences for the DN-to-pons ratio per group are displayed in Figure 2.

In the linear GBCA group, the mean DN-to-pons SI ratio difference of 0.0407 ± 0.0398 between the last and first examinations was significantly larger than 0 ($P <$ .001, 95% confidence interval [CI]: 0.0294, 0.0520), and the Bayes factor of 4214210 indicated strong support for the alternative hypothesis (difference from 0). In the macrocyclic GBCA group, the mean SI ratio difference of 0.0016 ± 0.0266 did not show a significant deviation from 0 (P = .680, 95% CI: −0.0060, 0.0091), and the Bayes factor of 0.17 indicated positive evidence for the null hypothesis (no difference from 0).

The mean SI ratio difference was significantly larger in the linear GBCA group than in the macrocyclic GBCA group ($P <$ .001, 95% CI: 0.0257, 0.0526) (Fig 3). The standardized difference between the two groups was d = 1.16, which corresponded to a large effect size. All previous results could be replicated by using the nonparametric equivalents (Wilcoxon signed rank and Mann-Whitney U tests).

When repeating the analyses for the DN-to-cerebellum ratio and the DN-to-CSF ratio, the results were comparable, with a difference that was significantly larger than 0 in the linear GBCA group (cerebellum, $P <$ .001, Bayes factor = 4070; CSF, $P <$ .001, Bayes factor = 2078), no significant difference from 0 in the macrocyclic GBCA group (cerebellum, P = .213, Bayes factor = 0.32; CSF, P = .143, Bayes factor = 0.43), and a significantly larger SI ratio difference in the linear GBCA group than in the macrocyclic GBCA group (cerebellum, $P <$ .001, d = 0.74; CSF, $P <$ .001, d = 0.89). However, the differences were strongest for the DN-to-pons ratio, which has been used both by Kanda et al (1) and Errante et al (2).

Figure 2

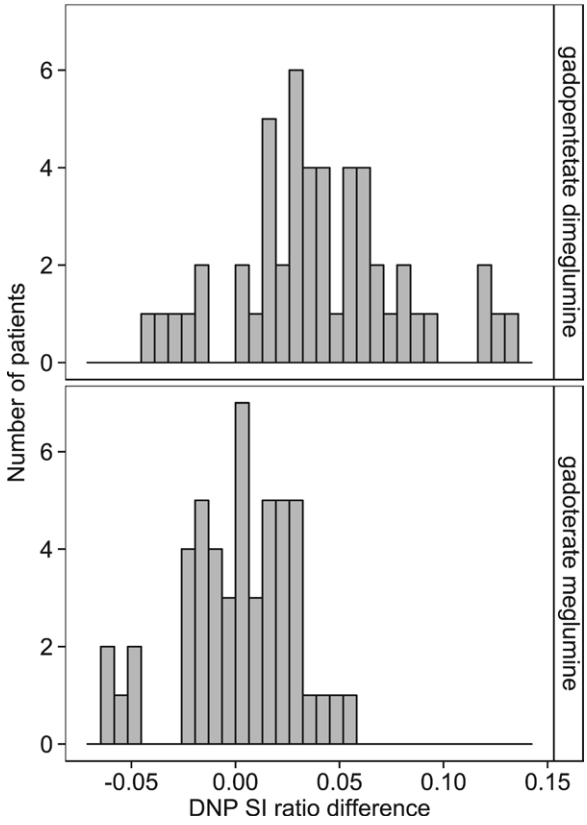

Figure 2: Graphs of the distribution of DN-to-pons *(DNP)* SI ratio differences between the last and first MR imaging examinations for the two patient groups.

Figure 3

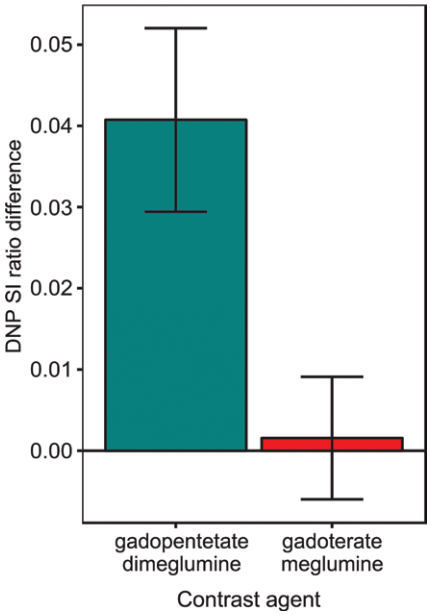

Figure 3: Graph of the mean DN-to-pons *(DNP)* SI ratio differences between the last and first MR imaging examinations for the two patient groups. Error bars represent the 95% CIs.

Table 3

Results of Linear Regression Analyses

Parameter	Regression Coefficient	95% CI	Standardized Regression Coefficient	*P* Value
First analysis				
Contrast agent	0.0424	0.0280, 0.0568	0.5462	<.0001
Age	0.0004	−0.0002, 0.0010	0.1463	.1952
Sex	0.0103	−0.0046, 0.0253	0.1320	.1733
History of chemotherapy				.9125
Molecularly targeted therapy	0.0021	−0.0164, 0.0206	0.0232	.8215
Alkylating antineoplastic agent	0.0009	−0.0198, 0.0215	0.0084	.9336
Other therapy	−0.0058	−0.0216, 0.0101	−0.0715	.4702
Underwent radiation therapy				.4952
Whole brain	0.0037	−0.0366, 0.0440	0.0187	.8555
Tumor selective	−0.0110	−0.0301, 0.0082	−0.1254	.2590
Diagnosis				.0565
Glioblastoma	0.0383	0.0020, 0.0747	0.2482	.0390
Glioma World Health Organization grade I–III	0.0365	0.0077, 0.0652	0.2608	.0135
Tumor other than glioma	−0.0220	−0.0679, 0.0238	−0.1004	.3423
eGFR	0.0008	−0.0199, 0.0214	0.0080	.9418
Abnormal liver function	0.0008	−0.0159, 0.0175	0.0094	.9224
Second analysis				
Contrast agent	0.0375	0.0246, 0.0504	0.4832	<.0001
No. of enhanced MR imaging examinations	0.0065	0.0023, 0.0107	0.2581	.0027
Third analysis				
Contrast agent	0.0382	0.0241, 0.0522	0.4918	<.0001
Mean interval between GBCA administrations	0.0004	−0.0011, 0.0018	0.0471	.6067
Fourth analysis				
Contrast agent	0.0466	0.0323, 0.0610	0.6013	<.0001
Accumulated dose of GBCA	0.0002	0.0000, 0.0004	0.2322	.0146

Note.—*P* values for sets of predictors were obtained by using hierarchical *F* tests.

The GP-to-thalamus ratio also showed comparable results. Consistent with Kanda et al (1), the GP-to-thalamus ratio difference was significantly larger than 0 in the linear GBCA group (0.0287 ± 0.0275; 95% CI: 0.0209, 0.0365; $P < .001$; Bayes factor = 6661 191). In line with the results for the DN, the ratio difference was not significantly different from 0 in the macrocyclic GBCA group (0.0031 ± 0.0354; 95% CI: −0.0069, 0.0132; $P = .538$; Bayes factor = 0.18). Finally, the difference was significantly larger in the linear GBCA group than in the macrocyclic GBCA group ($P < .001$, $d = 0.81$).

To control for the possibility that the difference between the two groups was due to other confounding variables, a linear regression analysis by using the DN-to-pons SI ratio difference as a criterion was performed. The results are summarized in Table 3. Even when controlling for a large number of variables, the effect of contrast agent on SI ratio difference remained highly significant ($P < .001$). The control variables sex, age, liver function, kidney function, diagnosis, chemotherapy, and radiation therapy did not have a significant influence on the SI ratio difference. The effect of contrast agent on SI ratio difference also remained highly significant ($P < .001$) when controlling for the number of contrast-enhanced MR imaging examinations, the accumulated dose of GBCA, and the mean interval between GBCA administrations in separate regression analyses.

The mean interval between GBCA administrations was not a predictor of a significant increase of the SI ratio difference, whereas both the number of contrast-enhanced MR imaging examinations and the accumulated dose of GBCA were. In additional analyses, we examined whether the respective correlation with the SI ratio difference was comparable for the linear GBCA group and the macrocyclic GBCA group or if it differed between groups.

In the linear GBCA group, the number of enhanced MR imaging examinations was positively related to an increase of the SI ratio difference ($r = 0.422$, $P = .002$), the Bayes factor of 11 indicating positive evidence for the alternative hypothesis (correlation different from 0). In the macrocyclic GBCA group, no significant relationship was found ($r = 0.015$, $P = .917$), with the Bayes factor of 0.11 indicating positive support for the null hypothesis (no correlation). A test for independent correlations indicated that the correlation in the linear GBCA group was significantly larger than the correlation in the macrocyclic GBCA group ($P = .035$).

The pattern of results was comparable when analyzing the relationship between accumulated dose of GBCA and SI ratio difference, with a significant correlation (r = 0.444, P = .001) and positive evidence for it (Bayes factor = 20) in the linear GBCA group but no significant correlation (r = 0.006, P = .967) and positive evidence for the null hypothesis (Bayes factor = 0.11) in the macrocyclic GBCA group. Likewise, these correlations differed significantly (P = .022). As in the overall regression analysis, the correlation between mean interval of GBCA administrations and SI ratio difference was not significant in both groups (linear GBCA group, r = 0.096, P = .506, Bayes factor = 0.14; macrocyclic GBCA group, r = −0.107, P = .460, Bayes factor = 0.15).

Finally, the independent-sample t test used to compare the T1-weighted sequences applied (magnetization-prepared rapid gradient-echo and spin-echo) in the linear GBCA group indicated that the sequence did not have a significant influence on the SI ratio difference (P = .770).

Figure 4 shows a typical finding before and after six administrations of a macrocyclic or linear GBCA.

Figure 4

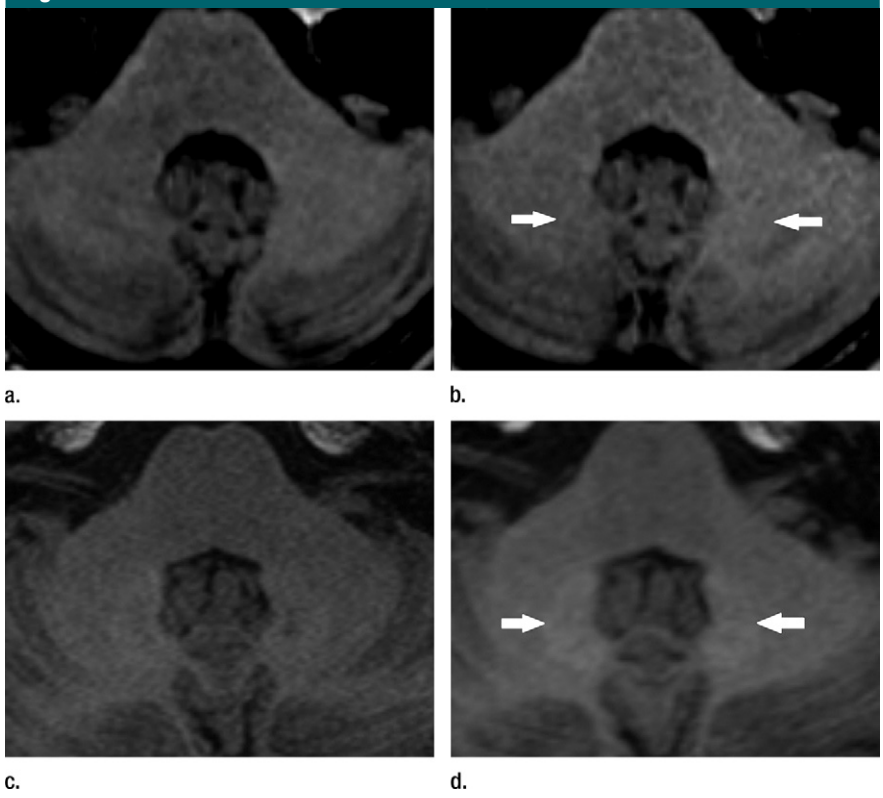

Figure 4: Unenhanced T1-weighted MR images of the typical finding of hyperintensities in the DN (arrows). Images were acquired **(a)** before and **(b)** after six administrations of macrocyclic GBCA and **(c)** before and **(d)** after six administrations of linear GBCA.

Discussion

In this study, we found an increased SI in the DN and GP on unenhanced T1-weighted images after serial applications of the linear GBCA gadopentetate dimeglumine, while no significant SI increase could be demonstrated for the macrocyclic GBCA gadoterate meglumine. Notably, this difference between the contrast agents was found, despite the fact that a substantially larger dose of contrast agent per MR imaging session was used in the macrocyclic GBCA group compared with the linear GBCA group. Furthermore, depending on the accumulated dose of GBCA, an increase of SI could be shown in the linear GBCA group, while no increase was found in the macrocyclic GBCA group.

These results confirm the findings of Kanda et al (3) for the applied linear GBCA gadopentetate dimeglumine and add further evidence that macrocyclic GBCA such as the assessed gadoterate meglumine does not cause an SI increase in the DN on unenhanced T1-weighted images; this latter finding was reported by Kanda et al (3) for the macrocyclic GBCA gadoteridol, but it is new for the GP.

Currently, it has not been proven that the SI increase in the DN or GP in patients with serial MR imaging examinations is caused by a deposition of gadolinium itself or by gadolinium-mediated changes, since histopathologic confirmation studies are not available yet. The hypothesis of gadolinium deposition exclusively caused by a linear GBCA, such as gadopentetate dimeglumine, is in line with theoretical considerations, as well as with findings from previous studies in which increased retention of a linear GBCA was reported in human bone, compared with a macrocyclic GBCA (7,11,12).

In a study by Kasahara et al (13), SI increase in the DN on nonenhanced T1-weighted images was described in patients treated with brain radiation. In contrast, neither whole-brain radiation nor tumor-selective radiation proved to be an independent confounder in our study. As noted by Errante et al (2) and Kanda et al (1), the total number of enhanced MR imaging examinations was not considered among the clinical variables in the study of Kasahara et al (13). Thus, the results of our study further support the theory that the reported SI increase on T1-weighted images by Kasahara et al (13) is caused by serial GBCA injections—frequently performed in patients after radiation therapy—rather than by the radiation therapy itself.

According to Errante et al (2) and contrary to Kanda et al (1), we excluded all patients with kidney dysfunction,

determined by an eGFR of less than 60 mL/min per square meter, to reduce the potential confounding effect of this parameter. Since gadoterate meglumine and gadopentetate dimeglumine are both exclusively excreted by the kidney, liver dysfunction was not taken as an exclusion criterion. However, the regression analysis demonstrated that abnormal liver function did not have an influence on SI increase.

Limitations of the current study are mostly caused by its retrospective design. Since patients were not randomly assigned to the different contrast agents, it cannot be ruled out that other confounding variables can explain the difference between the contrast agent groups; however, even when controlling for a large number of potentially confounding variables, the effect of the contrast agent group remained significant. Besides, the arbitrary number of six subsequent MR imaging examinations as an inclusion criterion was chosen to enable a comparison to the results of Kanda et al (1), who had initially chosen this cutoff criterion. We cannot exclude any previous exposure to a GBCA in life prior to the first analyzed MR images in our department. Therefore, potential prolonged retention of the prior gadolinium application cannot be ruled out as a possible confounder. However, the relatively homogeneous patient groups in our study make this scenario highly unlikely.

Furthermore, an autopsy study showed evidence for gadolinium accumulation in the pons (although the accumulation in the pons was weaker compared with the DN, GP, and thalamus) (14). To account for this, we repeated our analysis by using cerebellum and CSF as additional comparators. The results were comparable, although the differences between the two patient groups were largest when using the pons as comparator.

A further limitation of the study is that only two of the nine available GBCAs on the market have been analyzed. This approach was chosen because of the applied GBCAs in our department. Finally, we cannot exclude the fact that other properties of the assessed GBCAs besides the classification as either linear or macrocyclic contribute to the difference in SI increase. However, given the previously mentioned considerations about the different risk of gadolinium release for macrocyclic and linear GBCAs, taken together with the findings of Kanda et al (3) for the missing retention for the macrocyclic GBCA gadoteridol, this explanation seems highly likely. Future studies should include other GBCAs to finally solve this question.

As highlighted by Kanda et al (1), the mechanisms by which gadolinium causes SI increase in the DN remain unclear. Besides the retention of free gadolinium in the DN, a deposition of the entire molecule, including the complex, might be possible but unlikely, since the complex cannot cross an intact blood-brain barrier. Also, gadolinium-induced cell changes or a gadolinium metabolism of the DN might be hypothesized. Future studies with histopathologic correlations should clarify the pathophysiological mechanism. Furthermore, it is still unclear whether the potential gadolinium retention is also present in other parts of the human body. For example, it was already shown in animal experiments that liver and bone might be primary repository organs for gadolinium (15,16).

Ultimately and most importantly, it is still unknown whether the reported SI increase does have any clinical correlates. This might be investigated within future studies by conducting a thorough clinical and radiologic examination of patients who already presented increased SI in the DN after serial GBCA applications.

In conclusion, high signal intensities in the DN and GP were associated exclusively with the linear GBCA gadopentetate dimeglumine but not with the macrocyclic GBCA gadoterate meglumine. Future studies should be conducted to investigate whether this difference holds true for all linear and macrocyclic GBCAs.

Disclosures of Conflicts of Interest: A.R. Activities related to the present article: institution received a grant from Guerbet. Activities not related to the present article: author received payment from Abbvey for expert testimony and from Guerbet, Siemens, and Prime Oncology for lectures; author received payment from Guerbet, Abbvey, and Prime Oncology for travel accommodations. Other relationships: disclosed no relevant relationships. **L.D.W.** disclosed no relevant relationships. **P.J.K.** disclosed no relevant relationships. **O.E.** disclosed no relevant relationships. **S.B.** disclosed no relevant relationships. **P.K.** disclosed no relevant relationships. **S.H.** disclosed no relevant relationships. **W.W.** disclosed no relevant relationships. **H.P.S.** disclosed no relevant relationships. **M.B.** Activities related to the present article: author received a grant from Guerbet. Activities not related to the present article: author received grants from Novartis, Roche, Guerbet, Codman, Stryker, and Covidien; author received personal fees from Novartis, Roche, Guerbet, and Codman. Other relationships: disclosed no relevant relationships.

References

1. Kanda T, Ishii K, Kawaguchi H, Kitajima K, Takenaka D. High signal intensity in the dentate nucleus and globus pallidus on unenhanced T1-weighted MR images: relationship with increasing cumulative dose of a gadolinium-based contrast material. Radiology 2014;270(3):834–841.

2. Errante Y, Cirimele V, Mallio CA, Di Lazzaro V, Zobel BB, Quattrocchi CC. Progressive increase of T1 signal intensity of the dentate nucleus on unenhanced magnetic resonance images is associated with cumulative doses of intravenously administered gadodiamide in patients with normal renal function, suggesting dechelation. Invest Radiol 2014;49(10):685–690.

3. Kanda T, Osawa M, Oba H, et al. High signal intensity in dentate nucleus on unenhanced T1-weighted MR images: association with linear versus macrocyclic gadolinium chelate administration. Radiology 2015 Jan 27:140364. [Epub ahead of print]

4. Idée JM, Port M, Raynal I, Schaefer M, Le Greneur S, Corot C. Clinical and biological consequences of transmetallation induced by contrast agents for magnetic resonance imaging: a review. Fundam Clin Pharmacol 2006;20(6):563–576.

5. Port M, Idée JM, Medina C, Robic C, Sabatou M, Corot C. Efficiency, thermodynamic and kinetic stability of marketed gadolinium chelates and their possible clinical consequences: a critical review. Biometals 2008;21(4):469–490.

6. Frenzel T, Lengsfeld P, Schirmer H, Hütter J, Weinmann HJ. Stability of gadolinium-based magnetic resonance imaging contrast agents in human serum at 37 degrees C. Invest Radiol 2008;43(12):817–828.

7. Gibby WA, Gibby KA, Gibby WA. Comparison of Gd DTPA-BMA (Omniscan) versus Gd HP-DO3A (ProHance) retention in human bone tissue by inductively coupled plasma atomic emission spectroscopy. Invest Radiol 2004;39(3):138–142.

8. Aronen HJ, Gazit IE, Louis DN, et al. Cerebral blood volume maps of gliomas: comparison with tumor grade and histologic findings. Radiology 1994;191(1):41–51.

9. Rouder JN, Speckman PL, Sun D, Morey RD, Iverson G. Bayesian t tests for accepting and rejecting the null hypothesis. Psychon Bull Rev 2009;16(2):225–237.

10. Wetzels R, Wagenmakers EJ. A default Bayesian hypothesis test for correlations and partial correlations. Psychon Bull Rev 2012;19(6):1057–1064.

11. White GW, Gibby WA, Tweedle MF. Comparison of Gd(DTPA-BMA) (Omniscan) versus Gd(HP-DO3A) (ProHance) relative to gadolinium retention in human bone tissue by inductively coupled plasma mass spectroscopy. Invest Radiol 2006;41(3):272–278.

12. Maeda T, Goto H, Hara H, et al. Comparison of Gd-DTPA-BMA versus Gd-DOTA of gadolinium retention in human bone tissue with normal renal function [abstr]. In: Radiological Society of North America Scientific Assembly and Annual Meeting Program. Oak Brook, Ill: Radiological Society of North America, 2014; 161.

13. Kasahara S, Miki Y, Kanagaki M, et al. Hyperintense dentate nucleus on unenhanced T1-weighted MR images is associated with a history of brain irradiation. Radiology 2011;258(1):222–228.

14. McDonald RJ, McDonald JS, Kallmes DF, et al. Intracranial gadolinium deposition after contrast-enhanced MR imaging. Radiology 2015 Mar 5:150025. [Epub ahead of print]

15. Hals PA, Hogset A. Deposition of gadolinium after high and low doses of gadolinium chloride to mice: organ distribution, elimination and subcellular localization in liver cells [abstr]. In: Book of abstracts: Society of Magnetic Resonance in Medicine 1990. Berkeley, Calif: Society of Magnetic Resonance in Medicine, 1990; 1199.

16. Wedeking P, Tweedle M. Comparison of the biodistribution of 153Gd-labeled Gd(DTPA)2-, Gd(DOTA)-, and Gd(acetate)n in mice. Int J Rad Appl Instrum B 1988;15(4):395–402.